This article has been accepted for publication in a future issue of this journal, but has not been fully edited. Content may change prior to final publication. Citation information: DOI 10.1109/TCCN.2019.2929151, IEEE Transactions on Cognitive Communications and Networking

Performance Comparison of Alternative Indoor 5G Micro-Operator Deployments in 3.6 GHz and 26 GHz Bands

K. B. Shashika Manosha, K. Hiltunen†, M. Matinmikko-Blue, and M. Latva-aho
Centre for Wireless Communications, University of Oulu, Finland
†Ericsson Research, Oy L M Ericsson Ab, Finland
{manosha.kapuruhamybadalge, marja.matinmikko, matti.latva-aho}@oulu.fi
kimmo.hiltunen@ericsson.com

***Abstract*—The fifth generation (5G) networks will provide local high-quality wireless services, especially within indoor areas. New local 5G network operator models, such as the recently introduced micro-operators, are increasingly important for vertical specific service delivery. The emergence of 5G micro-operator networks in spatially confined areas depends on local spectrum availability. In this paper, we investigate the performance of local 5G indoor micro-operator networks in the 3.6 GHz and 26 GHz bands. We consider two uncoordinated TDD networks in adjacent buildings sharing the same channel with different base station antenna configurations and deployment densities. We evaluate the resulting performance of the victim network via system simulations. We have observed that the center frequency does not significantly impact the downlink performance unless the network is noise-limited. However, the uplink performance in 26 GHz band is affected by higher coupling losses between the base stations and mobile terminals. Our results indicate that beamforming and wider bandwidths help to improve the performance in 26 GHz band. More importantly, two indoor micro-operators can successfully coexist with a very small separation distance in the 26 GHz band, while in the 3.6 GHz band a considerably larger isolation between the networks is required, for example in the form of a much larger separation distance.**

***Index Terms*—5G, micro operator, radio network performance, throughput loss, spectrum access, 3.6 GHz band, 26 GHz band, system level simulations, coexistence**

I. Introduction

The fifth generation (5G) mobile communication networks are expected to facilitate a diverse set of use cases, which are key enablers of future digitalization [1]. These use cases have been broadly categorized as massive machine type communications, critical machine type communications, and enhanced mobile broadband [2]. Serving the various use cases is not an easy task due to their inherent requirements, such as guaranteed quality-of-service (QoS) levels (e.g., reliability and latency), enabling own management functionalities, and specific security standards [3].

Interestingly, the development of *local high-quality wireless networks* has started in standardization to allow the establishment of local 5G networks by different stakeholders to complement the traditional wide area networks deployed by the mobile network operators (MNOs) [3], [4]. Such a local high-quality network is expected to support the required QoS levels, privacy and security, and moreover, its operation is restricted to a spatially confined region to provide vertical specific services. In line with [3] and [4], the study in [5] has demonstrated that the QoS requirements related to the 5G use cases can be achieved by densified indoor networks. However, the success of these local networks will heavily depend on the availability of suitable spectrum bands for local operations with quality guarantees.

The micro-operator concept, recently proposed in the research domain, aims at enabling local high-quality 5G wireless networks to provide context related services and content to serve verticals especially indoors [6]–[8]. A micro-operator is a local and possibly venue specific service provider role that complements MNOs' offerings by deploying and operating local (small cell) networks. Different stakeholders can take the micro-operator role. As the micro-operators are expected to provide versatile high-quality services, it is necessary to provide guaranteed access to the spectrum with no or very limited harmful interference. One way to do this is via so called micro licensing model proposed in [9] for assigning local access rights [10] with an appropriate spectrum authorization framework [11]. Regulators are considering local spectrum access rights in the upcoming 5G spectrum decisions and some countries in Europe are in the process of defining rules for assigning local licenses in 3.6 GHz and 26 GHz bands following the opinions from the Radio Spectrum Policy Group (RSPG) of the European Commission (EC) in [12], [13]. Since licensing is a national level decision, the national regulators in Europe can award local spectrum licenses as long as they follow the European framework set by the and European Conference of Postal and Telecommunications administrations (CEPT) which are defined for the 3.6 GHz band in [14], [15], and 26 GHz band in [16], [17]. More information on recent 3.5 GHz spectrum awards is presented in [18]. Harmful interference between two micro-operators can be avoided by using an appropriate separation distance between these local license holders [19], [20], and the separation distance can be further reduced by managing the inter-operator interference [21]. For protecting the possible incumbents in the band, the authors in [4] have proposed a method based on an extension of the licensed shared access (LSA) for granting local access

This research has been financially supported by Business Finland in uO5G project and Academy of Finland in 6Genesis Flagship (grant 318927).

This article has been accepted for publication in a future issue of this journal, but has not been fully edited. Content may change prior to final publication. Citation information: DOI 10.1109/TCCN.2019.2929151, IEEE Transactions on Cognitive Communications and Networking

rights. Furthermore, the work in [22] verifies the technical feasibility of sharing the spectrum with incumbent users in LSA framework. All these works highlight the importance of facilitating guaranteed local access to the spectrum, by protecting the incumbent users in that band, to enable a large number local high-quality wireless networks.

In the starting point, 5G networks will be deployed in 700 MHz, 3.6 GHz, and 26 GHz bands in Europe [12]. While the 700 MHz band will mostly be used or is already being used in some countries for providing outdoor coverage through macro cells, the 3.6 GHz band will be targeted for both outdoor and indoor network deployments. On the other hand, the 26 GHz band will mainly be used for local networks including indoor deployments. Hence, by looking at the requirements of a micro-operator network (e.g., localized deployment and guaranteed QoS), it is clear that from the upcoming 5G bands both 3.6 GHz and 26 GHz are potential bands for deploying such a network by various stakeholders.

In response to regulators' initiatives, both industry and academia have been actively involved in preparing for the use of 3.6 GHz and 26 GHz bands by the 5G networks. For example, the FCC has introduced citizen broadband radio service (CBRS) to use the $3550 - 3700$ MHz band (named as 3.5 GHz band in the United States) for commercial usage [23]–[26]. In CBRS, a sharing based approach is used to allocate spectrum, and the sharing rules are defined based on the priority of the spectrum users [23], [24]. The successful operation of CBRS depends on the development of a suitable architecture [26] and the ability to coexist with the higher priority users (incumbents) in this band [27]–[30]. This model allows the establishment of micro operator networks through local priority access licenses (or under general authorization).

For millimeter wave bands, methods like spectrum pooling [31], [32], beam coordination [33], and inter-operator base station coordination [34] have been suggested to enable more efficient spectrum usage. On the other hand, the research community has also compared important channel parameters (e.g., path loss, delay spread, angular spread, etc.) [35]–[37] and cost-capacity performances [38] in the higher frequency bands. Furthermore, an interesting technical and economic study has been conducted in [39] to understand the implications of resource sharing in millimeter wave networks. There, the effect of available bandwidth, network density, and user density on the average and cell-edge throughput has been studied.

For efficient design and deployment of a wireless network, it is necessary to define suitable technical requirements such as carrier frequency, channel bandwidth, base station antenna type (omnidirectional or beamformed), block edge mask, etc. Then, an investigation is needed to identify the most appropriate combination of the above technical parameters resulting in the best network performance. This kind of investigation is important also in the case of a local high-quality network. However, to the best of our knowledge, none of the existing studies on 5G spectrum bands has investigated different deployment alternatives for local 5G micro-operator networks, and none has evaluated the impact of the selected deployment alternative on the performance of the network.

In this paper, we evaluate the feasibility of deploying local 5G high-quality wireless networks in the upcoming 3.6 GHz and 26 GHz bands. To do this, we consider a scenario with two uncoordinated 5G micro-operator networks located inside adjacent buildings. The micro-operator networks are assumed to use time division duplex (TDD) and they are assumed to be sharing the same channel in the absence of incumbent users or an overlaid co-channel outdoor network. During the system level performance evaluations we first consider a single-operator scenario and evaluate the performance of a few different deployment alternatives. Then, for a scenario with two adjacent micro-operators, we evaluate the impact of inter-operator interference on the average throughput losses in the downlink and uplink. The main contributions of this paper are as follows:

- We provide a comparison of different spectrum access models that can be used in 3.6 GHz or 26 GHz bands considering different stakeholders' perspectives including both MNOs and local entrant 5G micro operators.
- We evaluate the performance of a local indoor 5G micro-operator network, in terms of downlink and uplink throughput, that operates either in the 3.6 GHz or 26 GHz band, deployed to deliver local high-quality services, by conducting system level simulations.
- We quantify the benefits of using beamforming and wider channel bandwidths for the operation in 26 GHz band and compare with the performance in 3.6 GHz band.
- We evaluate the impact of co-channel inter-operator interference on the average performance in the downlink and uplink of the victim indoor operator network. We also test potential options (e.g., increasing victim network density, increasing channel bandwidth, etc.) to improve the performance of the victim network in the presence of co-channel interference.

One of the main assumptions for the co-existence evaluation in this paper is that the co-channel micro-operator networks are uncoordinated, which in practice means that the networks are allowed to apply different TDD patterns to satisfy their respective needs regarding both the offered traffic volume and the desired QoS. Furthermore, no interference coordination mechanisms between the micro-operators either on time, frequency, spatial or power domain are assumed. As discussed for example in [19]–[21], the obvious price of such uncoordinated TDD operation is the inter-network interference between the downlink and the uplink resulting in high isolation requirements between networks. By synchronizing the networks, the impact of the inter-network interference, and hence also the required level of isolation, can be reduced in particular for the clearly uplink-limited scenarios [40], but at the cost of a considerably reduced flexibility for the micro-operators to satisfy their service needs. Therefore, the approach chosen in this paper is to evaluate the performance of a few different deployment options, affecting both the level and the impact of the inter-network interference, to make the co-existence scenario between uncoordinated micro-operator TDD networks more feasible.

The rest of the paper is organized as follows. In Section II, we briefly discuss spectrum access options for allowing the

This article has been accepted for publication in a future issue of this journal, but has not been fully edited. Content may change prior to final publication. Citation information: DOI 10.1109/TCCN.2019.2929151, IEEE Transactions on Cognitive Communications and Networking

deployment of local 5G micro-operator networks. Section III introduces the system model, including the assumed network layout, propagation models and models for the radio resource management and user performance. Then, system simulation results are presented and analyzed in Section IV. Finally, some conclusions are drawn in Section V.

II. Spectrum Access Options for 5G Micro-Operator Networks

Timely availability of suitable spectrum with large enough bandwidths that support high throughput applications is seen as the key to ensure successful roll-out of 5G networks [15], [16], [41]. To facilitate this, the European regulators have released or intend to release up to 400 MHz bandwidth in 3.6 GHz band and 3.25 GHz bandwidth in 26 GHz band [12]. In many countries in Europe, these 5G bands are currently occupied by some incumbent spectrum users. Hence, the national regulators have to take appropriate actions to make 5G bands available by proposing migration plans to the incumbents or by enabling efficient coexistence techniques [41]. The other important role of the national regulators is to propose a suitable spectrum assignment model for defining and giving spectrum access rights to those requesting them including the determination of an appropriate geographic scope of spectrum licenses [42] according to their national situation. In the European level, the technical conditions for the use of the bands are presented in [14] for 3.6 GHz and in [17] for 26 GHz band, respectively.

The licensing scope defined in a spectrum assignment model can be either national, regional, or individual licenses, and at present, these models are being used by the regulators in Europe [41]. To allow the provisioning of local high-quality wireless services [3], the licensing scope of 5G would consider also the establishment of vertical specific 5G micro-operators which calls for regional or individual licenses. On the other hand, implementing local MNO deployed networks is also a potential approach to provide high-quality services. However, the successful operation of a local high-quality network depends on the availability of enough spectrum [12] to operate the network while guaranteeing the QoS required for the location and context specific services. To this end, it is essential that we compare the advantages and drawbacks of implementing MNO driven (local and nation wide) and local micro-operator driven networks in 3.6 GHz or 26 GHz bands, and identify appropriate deployment options and spectrum assignment models.

In Table I, we compare possible spectrum assignment models for 3.6 GHz or 26 GHz bands from the perspective of the MNOs and emerging local 5G micro-operators. The comparison considers both national and local spectrum assignment models. Furthermore, we assume that the MNOs can operate either in national or local level, and that the micro-operators operate only in local level. The signs used in the table for each evaluation criteria can be interpreted as follows: $+$ represents 'YES', $-$ represents 'NO', and $\backsim$ means neutral.

For both 3.6 GHz and 26 GHz bands, the regulatory burden is reduced when the spectrum is allocated in the national level in contrast to local level, since the number of MNOs that operate in national level in a country is very few and the complexity of licensing is reduced. This helps both the regulator and the licensee. On the other hand, when the licensing scope is local both MNOs and micro-operators can deploy their networks locally. Spectrum assignment for such local networks deployed by different stakeholders is creating an additional burden to the regulator, as it has to introduce a proper framework by well defining the key licensing elements, such as license area, awarding procedure, technical conditions, and mechanisms to handle interference.

Although the regulatory burden for assigning spectrum for micro-operators and local MNO networks can be high, the benefit of enabling such networks is that the stakeholders have an incentive to bid and operate in specific areas. In the case of nationwide license, MNOs often have obligations to provide nationwide coverage, and hence, they do not have the option of bidding and operating only in their desirable areas. Thus, there can be issues of guaranteeing the return of investment for the MNOs. However, local licenses do not pose such obligations, and hence, the local operators can bid and operate only in the areas of their interest. More importantly, the players do not need a large capital to take part in the license awarding procedure, and as a result, a larger number of players can enter the market.

If the regulator assigns spectrum only to the MNOs to deploy their networks both nationally and locally, this strictly prevents small players from entering to the market, which does not improve competition or promote innovation. This leads to the conventional approach, leaving only the traditional MNOs to obtain the licenses for a longer period of time, thus blocking the emergence of new players to the market with different business models. However, the concept of micro-operators is about allowing small players (with various business models) to emerge in both bands, thus enabling a competitive environment to enhance innovations in these bands. One drawback of enabling local licenses is the inability of providing nationwide services to the subscribers. In both bands, micro-operators cannot provide a nationwide service as they do not have a network that can cover the whole country. However, the MNOs who have local networks can facilitate this service, since they have national networks that guarantee the nationwide coverage.

As there are existing incumbent users in both 3.6 GHz and 26 GHz bands in some countries, the regulator should impose necessary conditions to guarantee efficient coexistence between the incumbents and MNOs as well as between the incumbents and potential micro-operators. The LSA concept that allows additional licensed users in bands, occupied by incumbents, is a way to introduce 5G networks to these bands as the additional licensed users. The coexistence between the incumbents and country wide MNOs in these two bands is a challenging tasks due to the obligations they have to fulfill. In the case of local MNOs and micro-operators that operate in 3.6 GHz band, an efficient coexistence can be achieved by managing the interference between the operators. To do this, methods like transmit power control and exclusion zones can be used. However, in the case of 26 GHz band the coupling

This article has been accepted for publication in a future issue of this journal, but has not been fully edited. Content may change prior to final publication. Citation information: DOI 10.1109/TCCN.2019.2929151, IEEE Transactions on Cognitive Communications and Networking

Table I
EVALUATION OF BANDS AND DEPLOYMENTS IN DIFFERENT STAKEHOLDERS' PERSPECTIVE.

Evaluation criteria	3.6 GHz			26 GHz		
	National	Local		National	Local	
	MNO	MNO	micro-OP	MNO	MNO	micro-OP
Additional regulatory burden	−	+	+	−	+	+
Incentive to bid and roll out in specific areas	−	+	+	−	+	+
Access to smaller players	−	−	+	−	−	+
Enable competition	−	−	+	−	−	+
Nationwide service	+	+	−	+	+	−
Efficient coexistence with Incumbents	−	∿	∿	−	+	+
Need for interference management	−	+	+	−	∿	∿

losses are much higher than in 3.6 GHz band. Hence, the interference generated towards the incumbent users is much smaller in 26 GHz band compared to 3.6 GHz band, thus enabling efficient coexistence with the incumbent users. More importantly, in cases where such coexistence is not feasible the regulator may restrict the operation of MNOs and micro-operators in that band. Nevertheless, compared to local MNO and micro-operator network deployment, nationwide MNO network deployment in these two bands is difficult.

Apart from protecting the incumbents in these two bands, necessary precautions must be taken to avoid any harmful interference generated by MNOs and micro-operators towards each other in the case of local licenses. The regulators generally issue orthogonal frequency bands for the MNOs (who operate nationally), and hence, by using the existing techniques the MNOs can efficiently manage the co-channel and adjacent channel interference in these two bands. In the case of local MNOs and micro-operators that operate in 3.6 GHz band, interference management is required as the coupling losses are lower. However, in the case of 26 GHz band the co-channel and adjacent channel interference is not difficult due to the higher coupling losses in this band.

The above evaluation concludes that the local deployment model for 5G is a promising approach to provide high-quality wireless networks in these two bands. In the remaining sections of this paper, we evaluate the technical feasibility of deploying a local indoor micro-operator network in the 3.6 GHz or 26 GHz band.

III. SYSTEM MODEL

This section provides a brief description of the considered network layout for a scenario with two neighboring 5G indoor micro-operators located inside adjacent buildings in the absence of incumbent spectrum users or an overlaid co-channel outdoor network. Furthermore, the applied propagation model for this deployment is presented. Finally, models for radio resource management and average user performance are introduced.

A. Network Layout

We consider an indoor deployment scenario with two TDD micro-operator networks are deployed inside adjacent buildings. The buildings are equally sized with dimensions 50×120 m, as defined in [43], and they are located at a distance D away from each other, as shown in Fig. 1. The buildings are assumed to be in line-of-sight (LOS) with each other and only one floor per building is modeled. We assume that micro-operator 1 (uO1) is serving the users within the first building, while micro-operator 2 (uO2) is serving the users within the second building. The users within both buildings are assumed to be uniformly distributed over the modeled floors.

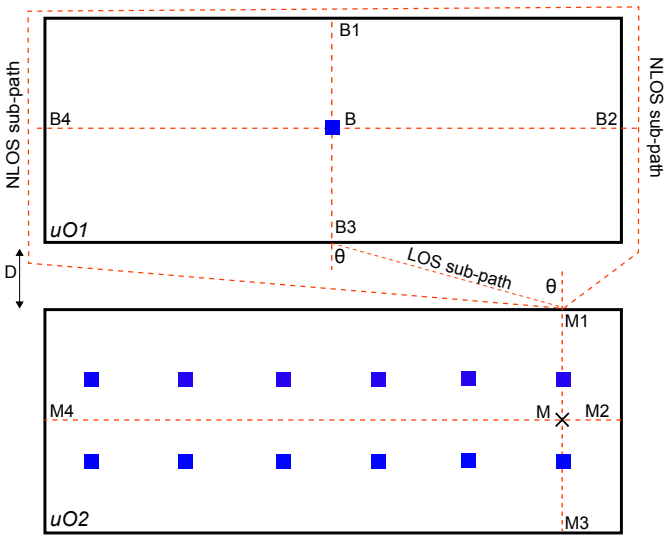

Figure 1. Considered network layout and the model for building to building propagation. The "square" marker is used to indicate a base station.

We assume that both networks are operating in the same channel either in 3.6 GHz or 26 GHz band. Furthermore, we assume that the base stations have either beamformed or omnidirectional antennas (see Fig. 2), and the mobile terminals have omnidirectional antennas.

B. Propagation Models

In order to model the propagation both within a micro-operator's network and between the neighboring micro-operators, we denote the absolute value of the coupling loss between base station b and mobile terminal m on beam n as C_{mbn} and that in decibel scale as $C_{mbn,\mathrm{dB}}$. The resulting coupling loss can be calculated as

$$C_{mbn,\mathrm{dB}} = L_{mb} - G_m^{\mathrm{ant}} - G_{bn}^{\mathrm{ant}} + X_{mb}, \qquad (1)$$

where L_{mb} is the path loss between mobile terminal m and base station b, G_m^{ant} is the antenna gain of mobile

This article has been accepted for publication in a future issue of this journal, but has not been fully edited. Content may change prior to final publication. Citation information: DOI 10.1109/TCCN.2019.2929151, IEEE Transactions on Cognitive Communications and Networking

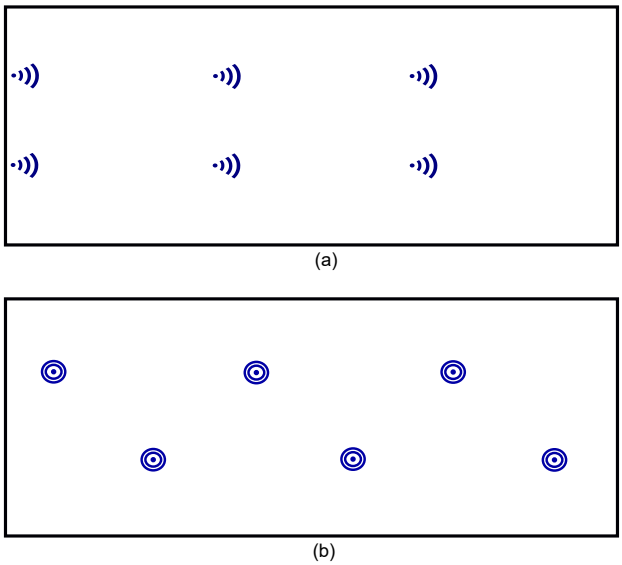

Figure 2. Base station deployment in a single floor of a micro-operator network: (a) with beamformed antennas (b) with omnidirectional antennas.

terminal m, G_{bn}^{ant} is the antenna gain of base station b on beam n, and X_{mb} denotes the log-normally distributed random value that models the impact of shadowing between mobile terminal m and base station b.

The mobile terminal antenna is assumed to be omnidirectional with antenna gain equal to 0 dBi. The base station antennas are assumed to be either omnidirectional or beamformed. In the case of omnidirectional antennas, the antenna gain is assumed to be equal to 5 dBi. In the case of beamformed base station antennas, we assume that the base station antenna consists of 4×16 cross-polarized antenna elements. Furthermore, analog beamforming is applied so that a grid of 48 different candidate beams are generated. These beams are generated within the range of approximately ± 55 degrees in azimuth and ± 13 degrees in elevation. The half-power beam width of each beam is approximately 8 degrees and the maximum antenna gain is equal to 23 dBi.

The indoor propagation within the floor is based on the 3GPP Indoor-Mixed Office propagation model defined in [43]. The path loss consists of both line-of-sight (LOS) and non-line-of-site (NLOS) components, and they are given by

$$L_{\text{LOS}} = 32.4 + 17.3 \log_{10}(d_{3D}) + 20 \log_{10}(f_c), \quad (2a)$$
$$L_{\text{NLOS}} = \max(L_{\text{LOS}}, L'_{\text{NLOS}}), \quad (2b)$$
$$L'_{\text{NLOS}} = 17.3 + 38.3 \log_{10}(d_{3D}) + 24.9 \log_{10}(f_c), \quad (2c)$$

where d_{3D} is the three-dimensional distance between the base station and the mobile terminal measured in meters and f_c is the center frequency in GHz. The LOS probability is given by

$$P_{\text{LOS}} = \begin{cases} 1 & d_{2D} \leq 1.2 \\ \exp(-\frac{d_{2D}-1.2}{4.7}) & 1.2 < d_{2D} \leq 6.5 \\ 0.32 \exp(-\frac{d_{2D}-6.5}{32.6}) & d_{2D} > 6.5, \end{cases} \quad (3)$$

where d_{2D} is the two-dimensional distance between the base station and the mobile terminal.

While modeling the impact of shadow fading, we assume that the standard deviation is equal to 3 dB in the case of LOS and 8 dB in the case of NLOS. Furthermore, we assume that the shadow fading and the LOS probability are spatially correlated with correlation distances equal to 10 m or 6 m (shadow fading in LOS or NLOS) and 10 m (LOS probability) [43].

To model the path losses between different buildings (i.e., building-to-building propagation), we evaluate four different sub-paths for each building, one through each building wall [44], as shown in Fig. 1. Hence, for each link between a transmitter and a receiver, the total received power is calculated as a linear sum of the received powers from all the 16 different sub-paths. For each sub-path, the outdoor path losses between the outer wall reference points B1-B4 and M1-M4 (see Fig. 1) and the building penetration and indoor losses for both buildings are taken into account to model the entire path loss. Thus, the path loss per sub-path is calculated as

$$L(f_c)_{\text{dB}} = L_{\text{in},1} + L_{\text{in},2} + L_{\text{ow},1}(f_c) + L_{\text{ow},2}(f_c) + L_{\text{out}}(f_c). \quad (4)$$

In (4), parameter L_{in} is the indoor loss modeled as $L_{in} = 0.5 d_{\text{2D-in}}$, where $d_{\text{2D-in}}$ is the two-dimensional distance between the indoor node and the outer wall reference point in meters [43]. Parameter L_{ow} is used to characterize the building wall loss and it consists of two parts: one that depends on the angle of incidence θ and the other that depends on the wall material and the center frequency f_c. Depending on the desired building penetration model, L_{ow} is calculated either as described in (5a) [45] or (5b) [43],

$$L_{\text{ow,LOS}} = 20(1 - \cos\theta)^2 + L_{\text{material}}(f_c), \quad (5a)$$
$$L_{\text{ow,NLOS}} = 5 + L_{\text{material}}(f_c), \quad (5b)$$

where $L_{\text{material}}(f_c)$ is the loss due to the used wall materials.

The building wall loss L_{ow} is calculated using (5a) for outer wall reference points B3 and M1 (see Fig. 1), and for the other outer wall reference points L_{ow} is calculated using (5b). The loss due to wall material $L_{\text{material}}(f_c)$ is obtained by using the model given in [43], and it assumes that the penetrated building wall loss consists of 30% multi-pane windows and 70% concrete in average.

Parameter L_{out} is the outdoor path loss between the outer wall reference points. In the case of LOS sub-path, i.e., the sub-path between B3 and M1 (see Fig. 1), L_{out} is calculated based on the free space propagation model, and the considered distance is the sum of the distances in the outdoor and indoor segments [44], [46]. In the case of NLOS sub-paths, L_{out} considers only the path between the outer wall reference points, and the path loss is calculated based on the recursive microcell model [47], with a breakpoint for the path loss exponent at 300 m. Finally, the shadow fading model assumes that the standard deviation is equal to 6 dB and the correlation distance is equal to 10 m. A more detailed description and analysis of the assumed building-to-building propagation model can be found in [19], [48].

This article has been accepted for publication in a future issue of this journal, but has not been fully edited. Content may change prior to final publication. Citation information: DOI 10.1109/TCCN.2019.2929151, IEEE Transactions on Cognitive Communications and Networking

C. Radio Resource Management and User Performance

In the system model, we assume that a user is served by only one base station using a single beam. The serving base station and the beam are chosen based on the coupling loss between the base station and the user terminal on that beam. We consider a round-robin scheduler operating in the time domain for scheduling users in both downlink and uplink. We assume that the network is applying dynamic TDD; the downlink and uplink slots are randomly selected to have a $50:50$ ratio in average. Furthermore, we assume that the base stations within the operator network are synchronized, which means that the downlink and uplink transmission do not overlap with each other. However, the base stations belonging to different micro-operators are assumed to be unsynchronized, which in practice means that when calculating the average user performance, each uplink (or downlink) slot will in average be interfered 50 percent of the time by uplink slots (transmissions from the mobile terminals) and the other 50 percent of the time by downlink slots (transmissions from the base stations) from the neighboring micro-operator.

The downlink signal-to-interference-plus-noise ratio (SINR) of mobile terminal m associated with base station b on beam n can be expressed as

$$\gamma_{mbn}^{\mathrm{DL}} = \frac{P_b^{\mathrm{BS}}}{C_{mbn}\left(I_{mb}^{\mathrm{own}} + I_m^{b2m} + I_m^{m2m} + N_m^{MT}\right)}, \tag{6}$$

where P_b^{BS} is the transmit power of bth base station, $N_m^{\mathrm{MT}}$is the thermal noise power of mth mobile terminal, C_{mbn} is the coupling loss between mobile terminal m and base station b on beam n. The notation I_{mb}^{own} denotes the inter-cell interference generated towards the mth user of base station b from all the other base stations of the serving micro-operator, I_m^{b2m} is the received interference from all the base stations, and I_m^{m2m} is the received interference from all the mobile terminals belonging to the other micro-operator. If beamformed antennas are used at the base stations, the intra- and inter-operator interferences, I_{mb}^{own}, I_m^{b2m}, and I_m^{m2m}, can be expressed as

$$I_{mb}^{\mathrm{own}} = \sum_{\substack{j=1\\ j\neq b}}^{J}\sum_{r=1}^{48}\frac{P_j^{\mathrm{BS}}\tau_{jr}}{C_{mjr}}, \tag{7a}$$

$$I_m^{b2m} = \epsilon_{d2d}\sum_{k=1}^{K}\sum_{r=1}^{48}\frac{P_k^{\mathrm{BS}}\tau_{kr}}{C_{mkr}}, \tag{7b}$$

$$I_m^{m2m} = \epsilon_{u2d}\sum_{k=1}^{K}\sum_{s=1}^{u_k}\frac{P_{sk}^{\mathrm{MT}}\tau_{sk}}{C_{ms}}. \tag{7c}$$

where τ_{jr} is an activity factor that indicates the probability (i.e., the average fraction of time) that beam r of base station j is being transmitted, and u_k is the number of uplink users simultaneously served by kth base station. Parameters ϵ_{d2d} and ϵ_{u2d} indicate the assumed inter-operator interference scenario. When it is DL-to-DL interference, $\epsilon_{d2d}=1$ and $\epsilon_{u2d}=0$, and in the case of UL-to-DL interference $\epsilon_{d2d}=0$ and $\epsilon_{u2d}=1$. In case of I_m^{m2m}, the notation τ_{sk} indicates the average probability that mobile terminal s served by kth base station is scheduled during an uplink slot.

For the base stations with omnidirectional antennas, the intra- and inter-operator interference levels are given by

$$I_{mb}^{\mathrm{own}} = \sum_{\substack{j=1\\ j\neq b}}^{J}\frac{P_j^{\mathrm{BS}}\tau_j}{C_{mj}}, \tag{8a}$$

$$I_m^{b2m} = \epsilon_{d2d}\sum_{k=1}^{K}\frac{P_k^{\mathrm{BS}}\tau_k}{C_{mk}}. \tag{8b}$$

where τ_j is the activity factor that indicates the probability that base station j is transmitting.

The uplink SINR of mobile terminal m served by base station b on beam n is given by

$$\gamma_{mbn}^{\mathrm{UL}} = \frac{P_{mbn}^{\mathrm{MT}}}{C_{mbn}\left(I_{bn}^{\mathrm{own}} + I_{bn}^{m2b} + I_{bn}^{b2b} + N_b^{\mathrm{BS}}\right)}, \tag{9}$$

where P_{mbn}^{MT} is the total transmission power of mobile terminal m associated with base station b on nth beam, N_b^{BS} is the thermal noise power of bth base station. The notations I_{bn}^{own}, I_{bn}^{m2b}, and I_{bn}^{b2b} are defined as follows:

$$I_{bn}^{\mathrm{own}} = \sum_{\substack{j=1\\ j\neq b}}^{J}\sum_{s=1}^{u_j}\frac{P_{sj}^{\mathrm{MT}}\tau_{sj}}{C_{sbn}}, \tag{10a}$$

$$I_{bn}^{m2b} = \epsilon_{u2u}\sum_{k=1}^{K}\sum_{s=1}^{u_k}\frac{P_{sk}^{\mathrm{MT}}\tau_{sk}}{C_{sbn}}, \tag{10b}$$

$$I_{bn}^{b2b} = \epsilon_{d2u}\sum_{k=1}^{K}\sum_{r=1}^{48}\frac{P_k^{\mathrm{BS}}\tau_{kr}}{C_{bnkr}}, \tag{10c}$$

where u_j is the set of uplink users associated with base station j, τ_{sj} is an activity factor that indicates the probability that the sth user of base station j is being scheduled for uplink transmission. In the case of UL-to-UL interference, $\epsilon_{u2u}=1$ and $\epsilon_{d2u}=0$, and for the DL-to-UL interference $\epsilon_{u2u}=0$ and $\epsilon_{d2u}=1$.

The total transmission power (in decibel scale) for mobile terminal m served by base station b on beam n is calculated as

$$P_{mbn,\mathrm{dBm}}^{\mathrm{MT}} = P_b^0 + 10\log_{10}(\beta) + \alpha_b C_{mbn,\mathrm{dB}}, \tag{11a}$$

$$P_{\min}^{\mathrm{MT}} \leq P_{mbn}^{\mathrm{MT}} \leq P_{\max}^{\mathrm{MT}}, \tag{11b}$$

where P_b^0 is the target for the received uplink power at the bth base station, β is the channel bandwidth, and α_b is the path loss compensation factor. The notations $P_{\min}^{\mathrm{MT}}$ and $P_{\max}^{\mathrm{MT}}$ define the minimum and maximum transmit powers of the mobile terminal, respectively. The uplink power control is in this paper assumed to be quite aggressive, aiming at fairly high P_b^0, while at the same time making sure that only a few users are transmitting at the maximum power. A higher P_b^0 allows the use of a higher modulation and coding scheme resulting in a higher uplink throughput. In addition, the uplink becomes also more tolerant of any inter-operator interference. Keeping the above in mind, it is straightforward to understand that the applied P_b^0 will in this study depend both on the assumed maximum coupling loss and channel bandwidth. In practice this means that P_b^0 can be increased together with the increased

This article has been accepted for publication in a future issue of this journal, but has not been fully edited. Content may change prior to final publication. Citation information: DOI 10.1109/TCCN.2019.2929151, IEEE Transactions on Cognitive Communications and Networking

base station density or when beamforming is applied, while P_b^0 has to be decreased as the center frequency or the channel bandwidth are increased.

The obtained SINR values can be mapped to corresponding user throughput values by using the following expression

$$R_{mb} = \frac{0.8\eta\beta \min\left(R_{\max}, \log_2(1+\gamma_{mb})\right)}{u_b}, \qquad (12)$$

where $\gamma_{mb} = \gamma_{mbn}^{\mathrm{DL}}$ for the downlink and $\gamma_{mb} = \gamma_{mbn}^{\mathrm{UL}}$ for the uplink. We assume that the average overhead due to control channels and data retransmissions is equal to 20%. Parameter η is used to indicate the average usage of the downlink and the uplink as a fraction of time. The maximum spectral efficiency $R_{\max}$ is defined by both the highest available modulation and coding rate and the maximum number of parallel data streams for each link. Furthermore, the effect of round-robin scheduling is taken into account via parameter u_b. Finally, if $\gamma_{mb} < -10$ dB we assume that $R_{mb} = 0$, otherwise R_{mb} is calculated by using (12).

IV. Evaluation Results

In this section, we first evaluate the impact of operating frequency bands, i.e., 3.6 GHz and 26 GHz, on the performance of a single indoor 5G micro-operator network, by using system level simulations. To do this, we compare the performance of three different deployment alternatives: 1) 3.6 GHz with omnidirectional base station antennas, 2) 26 GHz with omnidirectional base station antennas and 3) 26 GHz with beamformed base station antennas. For each of these deployment alternatives, we evaluate the average user throughputs in both downlink and uplink, by varying the base station density of the network, while keeping the total number of active users with full buffer traffic unchanged. The different deployment alternatives are then compared by evaluating the average user throughputs considering the same base station densities for all of them. Furthermore, the comparison is performed for both the noise-limited deployments with a low density of base stations and the more interference-limited deployments with a higher density of base stations. In the second part of the study, we evaluate the impact of inter-operator interference between two uncoordinated micro-operator networks located in adjacent buildings. Again, we assume that the micro-operators are operating either in 3.6 GHz or 26 GHz band, and they use the above mentioned alternatives to deploy their networks. Furthermore, we assume that both operators have selected the same deployment alternative. For each of the considered deployment alternatives, we evaluate the average throughput in downlink and uplink by varying the channel bandwidth, base station density of the victim and interfering operators, and the distance between the micro-operator buildings. The main simulation parameters are as listed in Table II. Furthermore, the parameters related to propagation, base station antenna array configuration, and base station deployment are presented in Sections III A, B and C.

Table II
Assumed parameter for the simulation.

Parameter	Value
Center frequency	3.6 GHz and 26 GHz
Channel bandwidths:	
• 3.6 GHz band	50 MHz
• 26 GHz	50 MHz and 200 MHz
Antenna heights:	
• Base station (BS)	3 m
• Mobile terminal (MT)	1 m
Transmit power:	
• BS transmit power	24 dBm
• MT maximum transmit power	23 dBm
• MT minimum transmit power	-40 dBm
Receiver noise figure	12 dB (BS), 9 dB (MT)
Antenna gains:	
• BS-beamforming	23 dBi
• BS-omni	5 dBi
• MT-omni	0 dBi
Maximum spectral efficiency	
• DL: 256 QAM, 2 streams	14.2 bps/Hz (DL)
• UL: 256 QAM, 1 stream	7.1 bps/Hz (UL)
Path loss compensation factor (α)	0.8
Number of users	10 (downlink) , 10 (uplink)
P_0 value:	
• 3.6 GHz-omni	-133 dBm
• 26 GHz-omni	-150 dBm
• 26 GHz-beamforming	-144 dBm

A. Scenario with a single micro-operator

We now evaluate the impact of the different deployment alternatives on the performance of a single 5G indoor micro-operator. Fig. 3(a) shows the normalized average downlink throughput and Fig. 3(b) shows normalized average uplink throughput versus the base station density for the different deployment alternatives. The results have been normalized with respect to the deployment that has 12 base stations in the 3.6 GHz band.

To start with, we discuss the impact of center frequency on the downlink performance. To do this, we compare the performance of a network operating at 3.6 GHz to the performance of a network operating at 26 GHz, assuming omnidirectional base station antennas and a channel bandwidth equal to 50 MHz for both of them. The results in Fig. 3(a) demonstrate that when the base station density is low, i.e., when the downlink SINR is noise-limited, the average throughputs observed in the 3.6 GHz band are slightly higher compared to the throughputs observed in the 26 GHz band. The downlink performance differences for the noise-limited deployments can be explained by the quite large coupling loss differences between the two frequency bands. More specifically, as indicated by (2) the coupling losses in the 26 GHz band are approximately $17-22$ dB higher compared to the 3.6 GHz band. However, as the base station density increases, the network is becoming more interference-limited, which means that the coupling losses have a smaller impact on the downlink SINRs, and further on the downlink user throughputs. Thus, in the end the downlink performance will become very similar for both frequency bands.

Next, we analyze the impact of channel bandwidth on the downlink performance by assuming deployment alternatives in the 26 GHz band with omnidirectional base station antennas. When the channel bandwidth is increased from 50 MHz to 200 MHz, the received power spectral density becomes

This article has been accepted for publication in a future issue of this journal, but has not been fully edited. Content may change prior to final publication. Citation information: DOI 10.1109/TCCN.2019.2929151, IEEE Transactions on Cognitive Communications and Networking

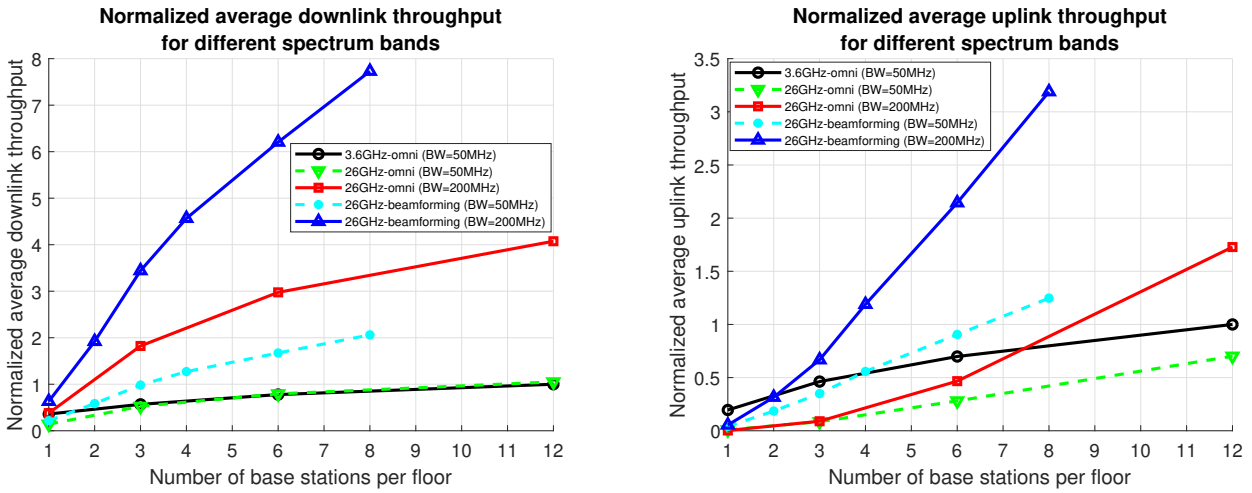

(a) (b)

Figure 3. Normalized average throughput versus the number of base stations for 3.6 GHz and 26 GHz bands: (a) downlink; (b) uplink.

lower, resulting in a lower downlink SINR for noise-limited deployments, and hence, a lower spectral efficiency. However, at the same time the average user throughputs are benefiting from the increased channel bandwidth (β), as indicated by (12). The obtained results in Fig.3(a) show that even the noise-limited sparse deployments benefit from the increased channel bandwidth, which means that the positive impact of increased channel bandwidth outweighs the negative impact of reduced spectral efficiency. In case of the more interference-limited dense deployments, the increased channel bandwidth has only a small negative impact on the downlink SINR, and therefore, a four-fold increase in the channel bandwidth results in a nearly four-fold increase in the observed downlink throughputs.

Finally, we analyze the impact of beamforming on the average and cell-edge downlink throughputs in the 26 GHz band. The results in Fig. 3(a) show that the average throughputs obtained with beamforming are considerably higher than the ones obtained with omnidirectional base station antennas. For the noise-limited network, beamforming helps to reduce the coupling losses compared to the deployments with omnidirectional base station antennas. When the network is interference-limited, the use of beamforming reduces both the coupling losses and in particular the level of the downlink inter-cell interference, because the active beams are quite often pointing away from the victim users. As a result, the use of beamforming helps to significantly improve the downlink throughputs for both the noise-limited and the interference-limited deployments.

To evaluate the impact of center frequency on the uplink performance, we compare the results in Fig. 3(b) for the 3.6 GHz and the 26 GHz band, assuming omnidirectional base station antennas and channel bandwidth equal to 50 MHz for both of them. The results show that the average throughput in the uplink is higher in the 3.6 GHz band compared to the 26 GHz for all the evaluated base station densities. These performance differences can be motivated by the higher coupling losses between the mobile terminals and the serving base stations, and consequently, the lower P_b^0 values applied for the 26 GHz band. For this particular case, the applied P_b^0 values are 17 dB lower for the 26 GHz band compared to the 3.6 GHz band, which corresponds to the coupling loss difference equal to 22 dB (for NLOS links) and path loss compensation factor equal to 0.8. Due to the lower P_b^0 values in the 26 GHz band, the users experience lower uplink SINR values, resulting in considerably worse uplink throughputs in particular for the noise-limited deployments. In case of the more interference-limited dense deployments, the impact of reduced P_b^0 on the uplink SINR becomes smaller, but there is still a clear performance difference in favor of the 3.6 GHz band. When it comes to the impact of channel bandwidth on the uplink performance, it is important to note that the applied P_b^0 values have to be scaled accordingly in order to maintain the same total transmission power levels for the mobile terminals. Hence, if the channel bandwidth is increased from 50 MHz to 200 MHz, the applied P_b^0 values have to be reduced by 6 dB. If the network is noise-limited, the uplink SINR is reduced by the same amount as the bandwidth is increased (i.e., by 6 dB in this case), while for the more interference-limited deployments the SINR is reduced somewhat less. From the average user throughput point of view, there is a trade-off between the increased channel bandwidth and the reduced SINR (i.e., the reduced spectral efficiency). However, as indicated by the obtained results, it is clearly beneficial to use a wider channel bandwidth, in particular when the network is dense enough to provide sufficient uplink coverage (SINR > -10 dB) throughout the evaluated floor area. As can be noticed, the average uplink throughput with 12 base stations and channel bandwidth equal to 200 MHz in the 26 GHz band is approximately 2.5 times as high as the corresponding throughput in the 3.6 GHz band with bandwidth equal to 50 MHz.

Finally, the use of beamforming reduces the coupling losses between the mobile terminals and the serving base stations, which allows higher P_b^0 values to be applied. For example, in these evaluations the difference compared to deployments with

This article has been accepted for publication in a future issue of this journal, but has not been fully edited. Content may change prior to final publication. Citation information: DOI 10.1109/TCCN.2019.2929151, IEEE Transactions on Cognitive Communications and Networking

omnidirectional antennas is in the range of $6-8$ dB. As a result of the higher P_b^0 values, the uplink SINRs and further the uplink throughputs are improved. Similar to the downlink, the use of beamforming reduces the level of inter-cell interference as well. However, since the uplink in the 26 GHz band is considerably less interference-limited compared to the downlink, the additional gain due to the reduced inter-cell interference is fairly small compared to the gain due to the increased P_b^0 values.

The performance of the different deployment alternatives for the single micro-operator case is summarized in Table III. The listed values indicate the minimum number of base stations required to achieve a similar performance in terms of the average throughput. In this comparison, the different deployment alternatives are benchmarked against a deployment in the 3.6 GHz band with omnidirectional base station antennas and channel bandwidth equal to 50 MHz.

Table III
MINIMUM NUMBER OF BASE STATION REQUIRED TO ACHIEVE SIMILAR PERFORMANCES IN DIFFERENT DEPLOYMENT ALTERNATIVES.

Deployment Alternative	**Number of base stations**	
	Downlink	**Uplink**
3.6 GHz-omni (BW = 50 MHz)	12	12
26 GHz-omni (BW = 50 MHz)	12	more than 12
26 GHz-omni (BW = 200 MHz)	2	9
26 GHz-beamforming (BW = 50 MHz)	3	7
26 GHz-beamforming (BW = 200 MHz)	2	4

Results in Table III indicate that the center frequency does not have any remarkable impact on the downlink performance of an interference-limited dense deployment. However, it does have a clear negative impact on the uplink performance. This is due to the fact that as a result of the applied uplink power control with fractional path loss compensation the uplink is less interference-limited compared to the downlink, and hence, the impact of the coupling loss difference between the evaluated bands is more visible. That is also the reason why the downlink benefits more from the increased channel bandwidth compared to the uplink. Finally, the values in Table III show that beamforming is highly beneficial for the performance of both the downlink and the uplink, in particular when combined with the additional channel bandwidth.

B. Scenario with two adjacent micro-operators

We now evaluate the performance of a scenario with two micro-operator networks deployed inside adjacent buildings, located as a default at a 25 m distance from each other. Here, we assume that micro-operator 1 is the victim operator and micro-operator 2 is the interfering operator (see Fig. 1). We evaluate the downlink and uplink average throughput losses within the victim network, which are obtained by comparing the user throughput values of the multi-operator scenario to the corresponding values within the single-operator scenario. The evaluation considers the impact of the building wall loss, channel bandwidth, density of the victim and the interfering network, and the separation distance between the buildings. Furthermore, similar to the single-operator scenario, three different deployment alternatives are considered: 1) 3.6 GHz with omnidirectional base station antennas, 2) 26 GHz with omnidirectional base station antennas and 3) 26 GHz with beamformed base station antennas.

1) Impact of interfering network density: Fig. 4 shows the average downlink and uplink throughput losses as a function of the base station density for the interfering micro-operator network. The victim network is assumed to have 3 BS/floor and the channel bandwidth is assumed to be 50 MHz for both networks. In order to study the impact of the density of the interfering network, let us first focus on the curves assuming omnidirectional base station antennas. It is clear that the average throughput losses for both the downlink and the uplink are increased as the density of the interfering network is increased. In case of downlink the increased performance losses are caused by the fact that when the base station density of the interfering network density increases, the number of simultaneously transmitting base stations (downlink-to-downlink interference) as well as the number of simultaneously transmitting mobile terminals (uplink-to-downlink interference) is increased, which leads to a higher level of inter-operator interference towards the victim network. Yet another reason explaining the increased level of the downlink inter-operator interference is the increased P_b^0 within the interfering network. As a result, both the downlink SINRs (see (6)) and the user throughputs become worse compared to the single-operator scenario.

In case of uplink, it is important to highlight that the main reason for the performance losses is the very high level of the interference between the base stations (downlink-to-uplink interference) as discussed already in [20]. Therefore, also the reasons for the observed performance losses together with the increased base station density of interfering network are very similar to the downlink: increased number of simultaneously transmitting base stations and mobile terminals, and the increased P_b^0 for the interfering network.

The results in Fig. 4 demonstrate that when the center frequency is increased from 3.6 GHz to 26 GHz the average throughput losses become much lower. This is due to the fact that the level of the inter-operator interference is reduced as a result of the increased path and building wall penetration losses: the building wall penetration loss increases from 7.7 dB to 12.4 dB [49], and at the same time the indoor and outdoor propagation losses become $17-22$ dB higher (see (2)). Finally, the results also show that the use of beamforming both within the victim and the interfering network reduces the impact of inter-operator interference even further, in particular for the higher values of the interfering network density. The reason for this is that the use of beamforming effectively reduces the average level of the received inter-operator interference. Moreover, in case of uplink the use of beamforming allows the use of slightly higher P_b^0 values, which makes the victim network more tolerant to external interference. In all, the results demonstrate that in case of 26 GHz the micro-operator buildings can be located close to each other without any major impact on the victim network performance. However, in case of 3.6 GHz, a similar co-existence performance requires

This article has been accepted for publication in a future issue of this journal, but has not been fully edited. Content may change prior to final publication. Citation information: DOI 10.1109/TCCN.2019.2929151, IEEE Transactions on Cognitive Communications and Networking

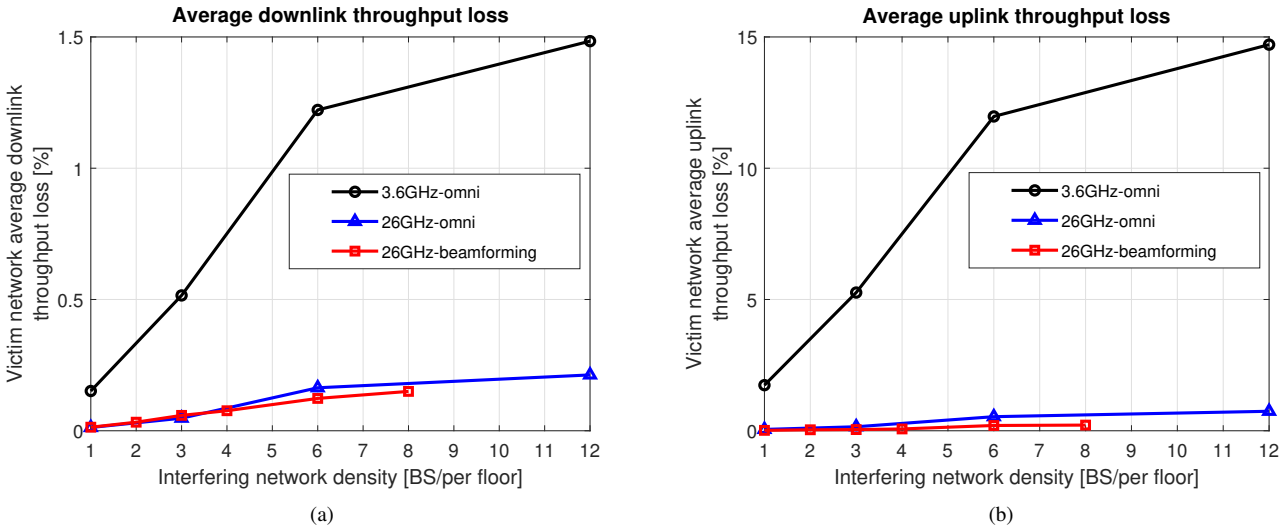

Figure 4. Average downlink and uplink throughput loss as a function of the base station density of the interfering network for the different deployment alternatives. The channel bandwidth is equal to 50 MHz, and victim network density is equal to 3 BS/floor.

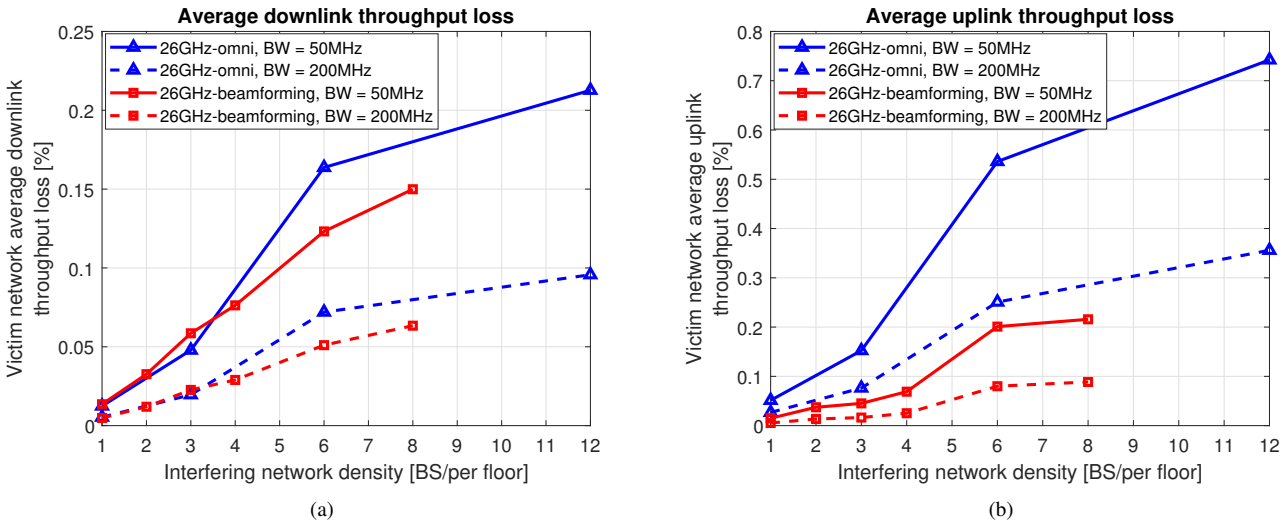

Figure 5. Average downlink and uplink throughput loss as a function of the base station density of the interfering network, assuming different channel bandwidths. The victim network density is equal to 3 BS/floor.

that the building walls have considerably higher penetration losses, for example as a result of the use of energy-efficient windows [48].

2) Impact of channel bandwidth: Fig. 5 shows the average downlink and uplink throughput losses of the victim network as a function of the base station density of the interfering network, assuming different channel bandwidths in the 26 GHz band. Again, the base station density for the victim network is assumed to be equal to 3 BS/floor. Results in Fig. 5(a) show that when the channel bandwidth is increased from 50 MHz to 200 MHz, the observed downlink throughput losses are reduced. This is due to fact that when the channel bandwidth is increased, the power spectral density of both the intra and the inter-operator interference are reduced, making the SINR more noise-limited and reducing the impact of inter-operator interference on the victim network performance.

Results in Fig. 5(b) show that as the channel bandwidth is increased from 50 MHz to 200 MHz, also the uplink throughput losses are reduced. The increased channel bandwidth has a negative impact on the uplink SNR since the P_b^0 has to be reduced by 6 dB in order to maintain the similar transmission power levels for the mobile terminals. Since also the interfering network will apply a lower P_b^0 due to the increased channel bandwidth the power spectral density of the inter-operator interference will become lower. As a result, the victim network becomes more noise-limited, and the impact of the inter-operator interference becomes smaller.

3) Impact of victim network density: Fig. 6 shows the average downlink and uplink throughput losses as a function of the base station density of the interfering network for the different deployment alternatives when the base station density of the victim network is increased from 3 to 6 BS/floor. Results in Fig. 6(a) show that the downlink throughput losses are reduced together with the increased base station density of

This article has been accepted for publication in a future issue of this journal, but has not been fully edited. Content may change prior to final publication. Citation information: DOI 10.1109/TCCN.2019.2929151, IEEE Transactions on Cognitive Communications and Networking

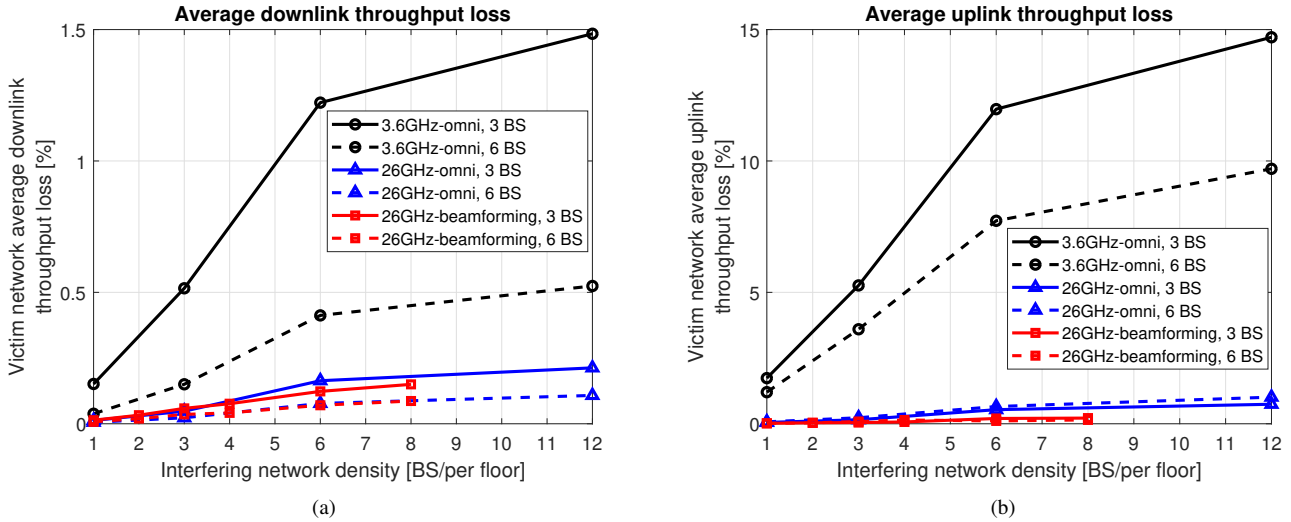

(a) (b)

Figure 6. Average downlink and uplink throughput loss as a function of the base station density of the interfering network, assuming different victim network densities. The channel bandwidth is equal to 50 MHz.

the victim network. With a higher density of base stations, the users within the victim network will experience both higher received power levels from the serving base stations, and a higher level of intra-operator interference. The latter is caused by the fact that the coupling losses towards the interfering base stations have become smaller, and at the same time the number of interfering base stations has increased. Since the level of the inter-operator interference stays the same, it will have a smaller impact on the downlink SINR and user throughputs. In case of 26 GHz band the level of the inter-operator interference is much lower compared to 3.6 GHz band and therefore the densification of the victim network has a smaller impact on the observed performance losses.

Fig. 6(b) depicts the uplink throughput losses as a function of the base station density of the interfering network. Similar to the downlink, the uplink performance losses become smaller when the base station density of the victim network is increased from 3 to 6 BS/floor. There are two main reasons for this: 1) a higher number of simultaneously active mobile terminals within the victim network and 2) an increased P_b^0 within the victim network, enabled by the reduced coupling losses between the mobile terminals and the serving base stations. As a result, both the level of the received carrier power and the level of the intra-operator interference increases. At the same time the level of the inter-operator interference is not affected, which means that it will have a smaller impact on the uplink SINR and the user throughputs.

4) Impact of the separation distance between the two buildings: In the previous simulations we have assumed that the distance between the micro-operator buildings is equal to 25 m. Now, if the separation distance between the buildings is increased, the corresponding average downlink and uplink throughput losses become smaller, as demonstrated by the results in Fig. 7. Specifically, in case of the 26 GHz band the coupling losses between the adjacent networks are so high that the throughput losses are very low even for the smaller separation distances. However, in case of the 3.6 GHz band there is a considerable throughput loss when the separation distance is smaller, especially in the uplink. For example, assuming that an average throughput loss up to 1% is allowed, the minimum separation distance becomes equal to 430 m for the 3.6 GHz band, while in case of the 26 GHz band the throughput loss is clearly less than the required 1% even when the buildings are located right next to each other.

V. Conclusions

In this paper, we have evaluated the suitability of upcoming 5G bands (3.6 GHz and 26 GHz) for the deployment of local indoor high-quality micro-operator networks. To do this, we have first compared different spectrum access options in these two bands for deploying local vertical specific 5G networks by either mobile network operators or micro-operators, and concluded that local deployment is a promising approach in both bands. Then, we have evaluated the downlink and uplink performance of two scenarios 1) single indoor micro-operator network and 2) two micro-operator networks in adjacent buildings via system simulations. In case of the single micro-operator scenario, we have observed that the performance of the downlink is not significantly affected by the center frequency, unless the system is noise-limited. However, in case of uplink the network performance in the 26 GHz band suffers from the considerably higher coupling losses between the base stations and the mobile terminals. We have also noticed that the network performance in the 26 GHz band benefit greatly from the use of both wider channel bandwidths and beamforming.

In the scenario with two adjacent micro-operator networks in adjacent buildings, we have observed that the throughput losses of the victim network increase as the base station density of the interfering network increases. Furthermore, we have seen that due to the lower coupling losses between the networks, the throughput losses are typically higher in the 3.6 GHz band than in the 26 GHz band. We have also noticed that the throughput losses within the victim network become

This article has been accepted for publication in a future issue of this journal, but has not been fully edited. Content may change prior to final publication. Citation information: DOI 10.1109/TCCN.2019.2929151, IEEE Transactions on Cognitive Communications and Networking

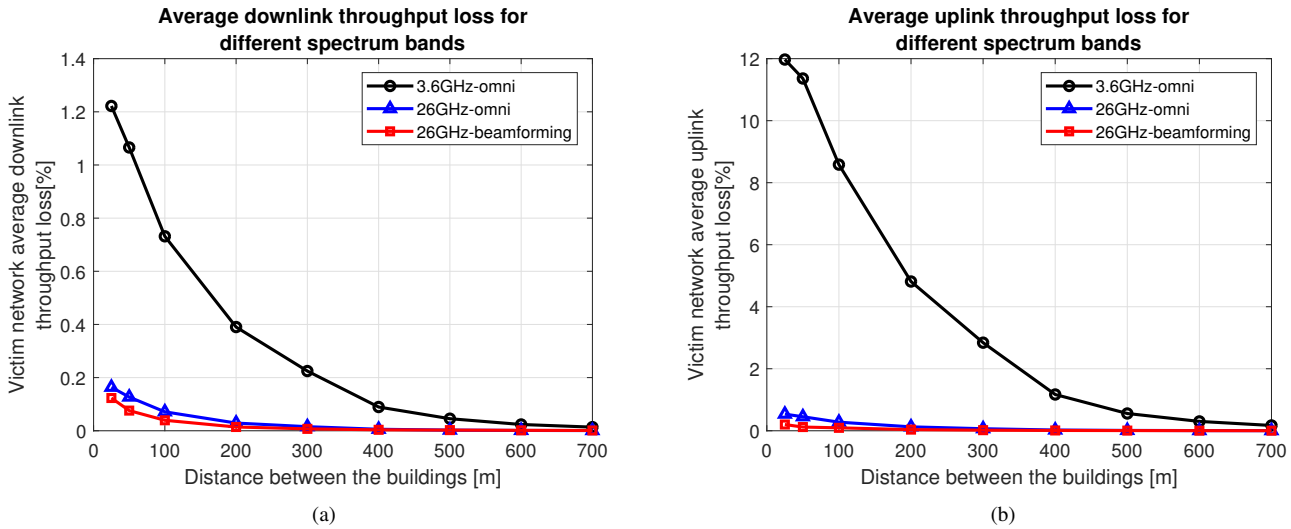

Figure 7. Average downlink and uplink throughput loss as a function of the separation distance. The channel bandwidth is equal to 50 MHz, the victim network density is equal to 3 BS/floor.

smaller with higher center frequency, the use of beamforming, higher building wall losses, wider channel bandwidths, denser victim network deployments and larger separation distances between the adjacent micro-operator buildings. In all, the results demonstrate that two indoor micro-operators can co-exist in the 26 GHz band with a very small separation distance between the buildings while having a very low performance loss. However, to achieve equally low performance losses also in the 3.6 GHz band the separation distance has to be considerably larger or the penetration losses of the building walls have to be higher.

We have so far assumed that the adjacent networks are deployed inside buildings. However, in case of future vertical specific 5G deployments, there could also be networks deployed outdoors. One interesting extension of our study is to evaluate the performance of two adjacent micro operator networks when base stations are also deployed outdoors leading to higher interference levels. Furthermore, in the countries where there are incumbent users occupying these bands, there is a need to consider the impact of local 5G networks on the incumbents which is easier to manage compared to nationwide deployments. In the future, it would also be interesting to extend our study to analyze the effect of uncoordinated incumbent transmission on the performance of local high-quality wireless networks.

Our study has also assumed that only the base stations operating in the 26 GHz band apply beamforming. In reality, beamforming would be feasible also for the 3.6 GHz band, improving the network performance compared to the deployment with omnidirectional antennas assumed in this paper. However, due to practical reasons (e.g., antenna size) the amount of antenna elements would be considerably smaller compared to the 26 GHz band, resulting in wider beams with lower antenna gains. Similarly, future studies could be enhanced by assuming that also the mobile terminals apply beamforming, in particular in the 26 GHz band. Finally, based on the results from previous studies related to for example LTE femtocell deployments [50], [51], LTE TDD interference management [52], [53], and the micro-operator co-existence evaluations presented in [21], it is quite evident that with the help of interference coordination the required level of isolation between the co-existing networks could be further reduced. This would be the case in particular for the 3.6 GHz band, where the interference between neighboring indoor networks clearly is an issue. Therefore, design and evaluation of feasible interference coordination mechanisms for micro-operator deployments would also be an interesting topic to be studied further.

REFERENCES

[1] 5GPP, "5G empowering vertical industries: roadmap paper," Tech. Rep., The 5G infrastructure public private partnership, 2016.
[2] Ericsson AB, "5G systems enabling transformation of industry and society," Tech. Rep., Jan. 2017.
[3] ETSI, "Feasibility study on temporary spectrum access for local high-quality wireless networks ETSI TR 103 588 version 1.1.1.)," Tech. Rep., The European Telecommunications Standards Institute, 2018.
[4] M. D. P. Guirao, A. Wilzeck, A. Schmidt, K. Septinus, and C. Thein, "Locally and temporary shared spectrum as opportunity for vertical sectors in 5G," *IEEE Network*, vol. 31, no. 6, pp. 24–31, Nov. 2017.
[5] J. Zander, "Beyond the ultra-dense barrier: Paradigm shifts on the road beyond 1000x wireless capacity," *IEEE Trans. Wireless Commun.*, vol. 24, no. 3, pp. 96–102, June 2017.
[6] M. Matinmikko-Blue, M. Latva-aho, P. Ahokangas, S. Yrjölä, and T. Koivumäki, "Micro operators to boost local service delivery in 5G," *Wireless Pers. Commun., Springer*, vol. 95, no. 1, pp. 69–82, July 2017.
[7] A. Prasad, Z. Li, S. Holtmanns, and M. A. Uusitalo, "5G micro-operator networks - a key enabler for new verticals and markets," in *Tel. Forum (TELFOR)*, Nov. 2017, pp. 1–4.
[8] M. G. Kibria, G. P. Villardi, K. Nguyen, W. S. Liao, K. Ishizu, and F. Kojima, "Shared spectrum access communications: A neutral host micro operator approach," *IEEE J. Select. Areas Commun.*, vol. 35, no. 8, pp. 1741–1753, Aug. 2017.
[9] M. Matinmikko-Blue, M. Latva-aho, P. Ahokangas, and V. Seppänen, "On regulations for 5G: Micro licensing for locally operated networks," *Els. Teleco. Policy*, vol. 42, no. 8, pp. 622–635, Sept. 2018.
[10] P. Anker, "From spectrum management to spectrum governance," *Els. Teleco. Policy*, vol. 41, no. 5, pp. 486 – 497, Sept. 2017.
[11] K. B. S. Manosha, M. Matinmikko-Blue, and M. Latva-aho, "Framework for spectrum authorization elements and its application to 5G micro-operators," in *Internet of Things Business Models, Users, and Networks*, Nov. 2017, pp. 1–8.

[12] ECC, "Strategic spectrum roadmap towards 5G for Europe, RSPG second opinion on 5G networks," Tech. Rep., Radio Spectrum Policy Group RSPG, RSPG18-005, 2018.

[13] RSPG, "RSPG opinion on 5G implementation challenges (RSPG 3rd opinion on 5G)," Tech. Rep., Radio Spectrum Policy Group Opinion, RSPG19-007 Final, 2019.

[14] ECC, "Harmonised frequency arrangements and least restrictive technical conditions (LRTC) for mobile/fixed communications networks (MFCN) operating in the band 3400-3800 MHz,," Tech. Rep., ECC Dec. (11)06, 2018.

[15] CEPT, "Review of the harmonized technical conditions applicable to the $3.4 - 3.8$ GHz ('3.6 GHz') frequency band," Tech. Rep., CEPT Report 67, 2018.

[16] ECC, "Harmonized technical conditions for mobile/fixed communication networks MFCN in the band $24.25 - 27.5$ GHz,," Tech. Rep., ECC Dec. (18)06, 2018.

[17] CEPT, "Harmonised technical conditions for the $24.25 - 27.5$ GHz ('26 GHz') frequency band," Tech. Rep., CEPT Report 68, 2018.

[18] M. Matinmikko-Blue, S. Yrjölä, V. Seppänen, P. Ahokangas, H. Hämmäinen, and M. Latva-aho, "Analysis of spectrum valuation elements for local 5G networks: Case study of 3.5-GHz band," *IEEE Cog. Commun. Net.*, 2019, Early access.

[19] K. Hiltunen, M. Matinmikko-Blue, and M. Latva-aho, "Impact of interference between neighbouring 5G micro operators," *Wireless Pers. Commun., Springer*, vol. 100, no. 1, pp. 127–144, May 2018.

[20] K. Hiltunen and M. Matinmikko-Blue, "Performance of neighboring indoor 5G micro operators with dynamic TDD," in *Proc. Eur. Conf. on Commun. and Networking*, June 2018, pp. 59–64.

[21] K. Hiltunen and M. Matinmikko-Blue, "Interference control mechanism for 5G indoor micro operator utilizing dynamic TDD," in *Proc. IEEE Int. Symp. Pers., Indoor, Mobile Radio Commun.*, Sept. 2018.

[22] D. Guiducci et.al., "Regulatory pilot on licensed shared access in a live LTE-TDD network in IMT band 40," *IEEE Cog. Commun. Net.*, vol. 3, no. 3, pp. 534–549, Sept. 2017.

[23] FCC, "Amendment of the commission's rules with regard to commercial operations in the 3550-3650 MHz band, Report and Order and Second Further Notice of Proposed Rulemaking," Doc.No. 12-354, Apr. 2015.

[24] FCC, "In the matter of promoting investment in the 3550-3700 MHz band," Doc.No. 17-258, Oct. 2018.

[25] M. M. Sohul, M. Yao, T. Yang, and J. H. Reed, "Spectrum access system for the citizen broadband radio service," *IEEE Commun. Mag.*, vol. 53, no. 7, pp. 18–25, July 2015.

[26] C. W. Kim, J. Ryoo, and M. M. Buddhikot, "Design and implementation of an end-to-end architecture for 3.5 GHz shared spectrum," in *Proc. IEEE Int. Symp. Dynamic Spectrum Access Networks*, Sept. 2015, pp. 23–24.

[27] N. N. Krishnan, R. Kumbhkar, N. B. Mandayam, I. Seskar, and S. Kompella, "Coexistence of radar and communication systems in CBRS bands through downlink power control," in *Proc. IEEE Military Commun. Conf.*, Oct. 2017, pp. 713–718.

[28] S. Kim, J. Choi, and C. B. Dietrich, "Coexistence between OFDM and pulsed radars in the 3.5 GHz band with imperfect sensing," in *Proc. IEEE Wireless Commun. and Networking Conf.*, Apr. 2016, pp. 1–6.

[29] T. T. Nguyen, A. Sahoo, M. R. Souryal, and T. A. Hall, "3.5 GHz environmental sensing capability sensitivity requirements and deployment," in *Proc. IEEE Int. Symp. Dynamic Spectrum Access Networks*, Mar. 2017, pp. 1–10.

[30] X. Ying, M. M. Buddhikot, and S. Roy, "Coexistence-aware dynamic channel allocation for 3.5 GHz shared spectrum systems," in *Proc. IEEE Int. Symp. Dynamic Spectrum Access Networks*, Mar. 2017, pp. 1–2.

[31] F. Boccardi, H. Shokri-Ghadikolaei, G. Fodor, E. Erkip, C. Fischione, M. Kountouris, P. Popovski, and M. Zorzi, "Spectrum pooling in mmwave networks: Opportunities, challenges, and enablers," *IEEE Commun. Mag.*, vol. 54, no. 11, pp. 33–39, Nov. 2016.

[32] M. Rebato, F. Boccardi, M. Mezzavilla, S. Rangan, and M. Zorzi, "Hybrid spectrum sharing in mmwave cellular networks," *IEEE Cog. Commun. Net.*, vol. 3, no. 2, pp. 155–168, June 2017.

[33] M. Nekovee, Y. Qi, and Y. Wang, "Distributed beam scheduling for multi-RAT coexistence in mm-wave 5G networks," in *Proc. IEEE Int. Symp. Pers., Indoor, Mobile Radio Commun.*, Sept. 2016, pp. 1–6.

[34] J. Park, J. G. Andrews, and R. W. Heath, "Inter-operator base station coordination in spectrum-shared millimeter wave cellular networks," *IEEE Cog. Commun. Net.*, pp. 1–1, Mar. 2018.

[35] Nokia, Nokia Shanghai Bell-Labs, 3GPP TSG RAN WG1 Meeting #94-bis, "Field measurement results from an operationa factory floor at 3.5 GHz and 28 GHz," Oct. 8-12 2018.

[36] A. O. Kaya, D. Calin, and H. Viswanathan, "28 GHz and 3.5 GHz wireless channels: Fading, delay and angular dispersion," in *Proc. IEEE Global Telecommun. Conf.*, Dec. 2017, pp. 1–7.

[37] F. Huang, L. Tian, Y. Zheng, and J. Zhang, "Propagation characteristics of indoor radio channel from 3.5 GHz to 28 GHz," in *Proc. IEEE Veh. Technol. Conf.*, Sept. 2016, pp. 1–7.

[38] V. Nikolikj and T. Janevski, "A comparative cost-capacity modeling of wireless heterogeneous networks, implemented within the 0.7 GHz, 2.6 GHz, 5 GHz and 28 GHz bands," in *Int. Conf.on Ultra-WideBand*, Sept. 2014, pp. 489–494.

[39] F. Fund, S. Shahsavari, S. S. Panwar, E. Erkip, and S. Rangan, "Spectrum and infrastructure sharing in millimeter wave cellular networks: An economic perspective," [Online]. Available: https://arxiv.org/abs/1605.04602, 2016.

[40] K. Hiltunen, M. Matinmikko-Blue, and M. Latva-aho, "Interference between 5G indoor micro operators utilizing beamforming and dynamic TDD in 26 GHz band," IEEE Wireless Commun. and Networking Conf., 2019.

[41] ECC, "Guidance on defragmentation of the frequency band 3400-3800 MHz," Tech. Rep., ECC Report 287, 2018.

[42] ECC, "Radio spectrum policy group report on assignment and pricing methods," Tech. Rep., Radio Spectrum Policy Group RSPG, RSPG 09-298, 2009.

[43] 3GPP; Technical Specification Group Radio Access Network, "Study on channel model for frequencies from 0.5 GHz to 100 GHz (3GPP TR 38.901 version 14.1.1.)," Tech. Rep., 3rd Generation Partnership Project (3GPP), 2017.

[44] E. Damasso and L. M. Correia (ed.), "COST 231 final report: Digital mobile radio towards future generation systems," Tech. Rep., COST 231, 1999.

[45] E. Semaan, F. Harrysson, A. Furuskär, and H. Asplund, "Outdoor-to-indoor coverage in high frequency bands," in *Proc. IEEE Global Telecommun. Conf. Workshop*, Dec. 2014, pp. 393–398.

[46] J. E. Berg, "Building penetration loss along urban street microcells," in *Proc. IEEE Int. Symp. Pers., Indoor, Mobile Radio Commun.*, Oct. 1996, vol. 3, pp. 795–797.

[47] J. E. Berg, "A recursive method for street microcell path loss calculations," in *Proc. IEEE Int. Symp. Pers., Indoor, Mobile Radio Commun.*, Sept. 1995, vol. 1, pp. 140–143.

[48] K. Hiltunen and M. Matinmikko-Blue, "Propagation model for evaluating the interference between neighboring indoor micro operators," in *Proc. IEEE Veh. Technol. Conf.*, June 2018.

[49] ITU, "Compilation of measurement data relating to building entry loss," Tech. Rep., ITU-R P.2346-2, 2017.

[50] 3GPP; Technical Specification Group Radio Access Network, "TDD home eNodeB (HeNB) radio frequency (RF) requirements analysis (3GPP TR 36.922 version 15.0.0.)," Tech. Rep., 3rd Generation Partnership Project (3GPP), 2018.

[51] L. G. Uzeda Garcia, I. Z. Kovacs, K. I. Pedersen, G. W. O. Costa, and P. E. Mogensen, "Autonomous component carrier selection for 4G femtocells - A fresh look at an old problem," *IEEE J. Select. Areas Commun.*, vol. 30, no. 3, pp. 525–537, Apr. 2012.

[52] 3GPP; Technical Specification Group Radio Access Network, "Further enhancements to LTE time division duplex (TDD) for downlink-uplink (DL-UL) interference management and traffic adaptation (3GPP TR 36.828 version 11.0.0.)," Tech. Rep., 3rd Generation Partnership Project (3GPP), 2012.

[53] Z. Shen, A. Khoryaev, E. Eriksson, and X. Pan, "Dynamic uplink-downlink configuration and interference management in TD-LTE," *IEEE Commun. Mag.*, vol. 50, no. 11, pp. 51–59, Nov. 2012.

K. B. Shashika Manosha received the B.Sc.(Eng.) degree in electrical and information engineering from the University of Ruhuna, Matara, Sri Lanka, in 2007, the M.Eng. degree in information and communication technologies from the Asian Institute of Technology, Thailand, in 2010, and the Dr.Sc.(Tech.) degree in Telecommunications Engineering from the University of Oulu, Finland in 2018. Currenly, he is working as an R & D engineer in channel modelling and solutions team in Keysight Technologies, Oulu, Finland. His research interests include massive MIMO communications, wireless channel modelling and OTA, spectrum sharing, and application of optimization techniques for wireless communications.

This article has been accepted for publication in a future issue of this journal, but has not been fully edited. Content may change prior to final publication. Citation information: DOI 10.1109/TCCN.2019.2929151, IEEE Transactions on Cognitive Communications and Networking

Kimmo Hiltunen received his M.Sc. (Tech) degree from Helsinki University of Technology, Finland, in 1996, and his D.Sc. (Tech) degree from Aalto University, Finland, in 2014. During 1998-2017 he worked at Ericsson Research, Wireless Access Networks, both in Finland and in Sweden. Since 2005 he holds a position as a Senior Specialist within the area of dense and heterogeneous network deployments. In 2017-2018, Kimmo Hiltunen worked as a senior research fellow at University of Oulu, Centre for Wireless Communications (CWC), focusing on 5G and the performance of micro operator deployments. He returned to Ericsson in 2018.

Marja Matinmikko-Blue is Senior Research Fellow and Adjunct Professor in Spectrum Management at Centre for Wireless Communications (CWC), University of Oulu. Prior to joining CWC, she worked at VTT Technical Research Centre of Finland Ltd. in 2001-2015. She holds a Dr.Sc. (Tech.) degree in Telecommunications Engineering from University of Oulu on cognitive radio techniques, and a Ph.D. degree in Industrial Engineering and Management on stakeholder analysis for spectrum sharing. In 2016-2018 she managed uO5G project that proposed a new micro operator concept. Currently she is Research Coordinator 6G Flagship - Finnish Wireless Flagship for 2018-2026. She conducts interdisciplinary research on future mobile communication networks from business, technical, and regulatory perspective in close collaboration with industry, academia, and regulators. She has published over 120 scientific papers and prepared 100 contributions to spectrum regulatory forums in Europe (CEPT) and globally (ITU).

Matti Latva-aho received the M.Sc., Lic.Tech. and Dr. Tech (Hons.) degrees in Electrical Engineering from the University of Oulu, Finland in 1992, 1996 and 1998, respectively. From 1992 to 1993, he was a Research Engineer at Nokia Mobile Phones, Oulu, Finland after which he joined Centre for Wireless Communications (CWC) at the University of Oulu. Prof. Latva-aho was Director of CWC during the years 1998-2006 and Head of Department for Communication Engineering until August 2014. Currently he serves as Academy of Finland Professor in 2017-2022 and is Director for 6G Flagship - Finnish Wireless Flagship for 2018-2026. His research interests are related to mobile broadband communication systems and currently his group focuses on 5G and beyond systems research. Prof. Latva-aho has published 350+ conference or journal papers in the field of wireless communications. He received Nokia Foundation Award in 2015 for his achievements in mobile communications research..